Sensors and Materials, Vol. 38, No. 2 (2026) 515–520
MYU Tokyo

S & M 4314

Comparison of Scintillation Performance of $Ca_3TaGa_3Si_2O_{14}$ and $Ca_3TaAl_3Si_2O_{14}$ Single Crystals

Ryosei Takahashi,* Kai Okazaki, Daisuke Nakauchi,
Takumi Kato, Noriaki Kawaguchi, and Takayuki Yanagida

Nara Institute of Science and Technology (NAIST), 8916-5 Takayama-Cho Ikoma, Nara 630-0192, Japan

(Received October 23, 2025; accepted December 11, 2025)

Keywords: scintillator, CTGS, CTAS, radiation detection

$Ca_3TaGa_3Si_2O_{14}$ (CTGS) and $Ca_3TaAl_3Si_2O_{14}$ (CTAS) single crystals were grown by the floating zone method, and their photoluminescence and scintillation properties were investigated. The CTGS and CTAS samples showed broad emission bands at 300–600 nm under UV light and X-rays, and the decay time constants were of ms order. From the afterglow curves after X-ray irradiation for 2 ms, the afterglow levels at 20 ms were 30 ppm for CTGS and 40 ppm for CTAS. The pulse height spectra of ^{137}Cs γ-rays measured using the CTGS and CTAS demonstrated that the calculated light yields of CTAS and CTGS were 1200 and 600 photons/MeV, respectively.

1. Introduction

Scintillators are functional materials that emit ultraviolet or visible light upon excitation by ionizing radiation. Combined with photodetectors, they are widely used in radiation detection for applications such as medicine,[1,2] security,[3,4] and resource exploration.[5,6] For X- and γ-ray detections, ideal scintillators should have high scintillation intensities, high density (ρ), large effective atomic number (Z_{eff}), and low afterglow level (*AL*). However, there are no scintillators that me*et all* the requirements; hence, application-specific scintillators have been developed in various material forms, including crystals,[7–10] ceramics,[11–13] and glasses.[14–17]

Scintillation detectors are categorized into integrated type and pulse counting type. In the former, scintillation signals are converted into electrical signals by photodetectors, and the signals are accumulated in several tens of milliseconds to seconds. They have been applied in X-ray computed tomography and baggage inspection at airports. Tl-doped CsI and $CdWO_4$ (CWO) are representative scintillators for the applications. They have some advantages such as high light yield (*LY*) in Tl-doped CsI and high interaction cross sections with X-rays and good *AL* in CWO. However, Tl-doped CsI suffers from its high *AL*, and CWO shows toxicity owing to the presence of Cd. Therefore, developments of new scintillators with high *LY*, low *AL*, and low toxicity have been desired.

*Corresponding author: e-mail: takahashi.ryosei.tn7@naist.ac.jp
https://doi.org/10.18494/SAM6018

ISSN 0914-4935
https://myukk.org/

To meet the demands, Ta-based oxide compounds have been proposed in recent years. Ta is a nontoxic element, and several Ta-containing compounds such as $Zn_3Ta_2O_8$ (26000 photons/MeV), $YTaO_4$ (15200 photons/MeV), and $Mg_4Ta_2O_9$ (19900 photons/MeV) have been reported to exhibit high *LY* values.[18] Among them, langasite-type compounds incorporating Ta have attracted attention not only for their promising properties but also their favorable synthesis characteristics. In particular, their relatively low melting points compared with other Ta-based oxides make them compatible with scalable crystal growth, which is advantageous for industrialization. In our previous studies,[19,20] we demonstrated that the $Ca_3TaGa_3Si_2O_{14}$ (CTGS) langasite type exhibited a better afterglow performance than Tl-doped CsI,[21] although the *LY* was inferior to those of CWO and Tl-doped CsI.[22] To explore new langasite-type scintillators with improved *LY* while maintaining low *AL*, we focused on $Ca_3TaAl_3Si_2O_{14}$ (CTAS), in which Ga is replaced with Al. CTAS is expected to offer high crystal quality owing to the absence of volatile elements such as Ga. High-quality crystals are advantageous for scintillation properties as they typically contain fewer defects and cracks that can quench luminescence or hinder energy transfer. Despite previous reports on the photoluminescence (PL) properties of CTAS,[23] its scintillation properties remain unexplored. In this study, CTAS single crystals were synthesized by the floating zone (FZ) method, and their PL and scintillation properties were investigated. Although many scintillators with dopants have been reported in previous studies, undoped CTAS was selected in this study with the expectation of obtaining higher-quality crystals than CTGS. In addition, undoped CTGS single crystals were synthesized by the same method to investigate the effects of element substitution on the PL and scintillation.

2. Materials and Methods

The CTGS and CTAS single crystals were synthesized by the FZ method. CaO (4N), Ta_2O_5 (4N), Ga_2O_3 (4N), Al_2O_3 (4N), and SiO_2 (4N) were used as raw materials. They were mixed using a mortar and a pestle. After that, they were formed into rods. The rods were sintered in an electric furnace (NHK-170, Nitto Kagaku) at 1200 °C for the CTGS samples and 1400 °C for the CTAS samples, each for 8 h. The sintered rods were set into a FZ furnace with four xenon arc lamps (FZ-T-12000-X-VPO-PC-YH, Crystal Systems),[24] and crystal growth was conducted. The crystalline rods were cut and polished for the following PL and scintillation measurements.

The crystal structures of the synthesized samples were analyzed by measuring the powder X-ray diffraction (XRD) patterns using an X-ray diffractometer (MiniFlex600, Rigaku). PL excitation and emission spectra were measured with a spectrofluorometer (FP-8600, Jasco), and PL quantum yields (*QY)* were obtained with a Quantaurus-QY spectrometer (C11347, Hamamatsu Photonics). Scintillation spectra, scintillation decay curves, afterglow curves, and pulse high spectra (PHS) of ^{137}Cs γ-rays (662 keV) were measured using lab-made devices.[25,26] To measure PHS, a photomultiplier tube (PMT, R7600U-200, Hamamatsu Photonics), a preamplifier (Model 113, ORTEC), a shaping amplifier (Model 570, ORTEC), and a multichannel analyzer (Pocket MCA 8000A, Amptek) were used. $Bi_4Ge_3O_{12}$ (BGO, *LY*: 8200 photons/MeV, 5 × 5 × 5 mm^3, Saint Gobain) was used as a reference sample to evaluate the *LY* of the prepared samples. Here, shaping times in CTGS, CTAS, and BGO were 10, 10, and 3 μs, and gains were 500, 500, and 100, respectively.

3. Results and Discussion

Figure 1 shows a photograph of CTGS and CTAS after cutting and polishing, with thicknesses of ~1 mm. Both samples appear colorless and transparent. The XRD patterns of the prepared samples and reference patterns [International Centre for Diffraction Data (ICDD): 00-052-1682 for CTGS, 00-051-0181 for CTAS] are also shown in Fig. 1. The patterns agreed with the reference data, confirming that both samples have a langasite-type structure belonging to the trigonal system with the space group of *P*321.[27,28]

Figure 2 shows the PL excitation and emission spectra. PL excitation spectra were measured when monitoring at 440 nm. CTGS exhibited an excitation band with two peaks at 200–300 nm, while CTAS showed an excitation band at 230 nm. The origin of their peaks is considered to be related to F centers at 250 nm and self-trapped excitons (STEs) at 230 nm.[29] Moreover, both samples showed emission bands at 300–600 nm upon excitation at 250 nm. The emission from CTGS was attributed to F centers (440 nm) and STEs (330 nm) because a similar spectral feature was reported previously.[29] The emission band in CTAS at 300–600 nm was similar to the previously reported PL,[23] and the spectral shape of CTAS was also similar to those previously reported for CTGS,[29] suggesting the same emission origin. The *QY*s under excitation at 250 nm were determined to be 4.3% for CTGS and 3.3% for CTAS.

The scintillation spectra of CTGS and CTAS under X-ray irradiation are shown in Fig. 3. Both samples showed emission peaks at 300–600 nm, and the spectra were similar to those of the PL spectra; hence, the origin can be similar to that of the PL emissions (330 nm emission: STE; 400 nm emission: F center). Moreover, the 440 nm emission band under UV excitation shifted to 400 nm under X-ray irradiation. A similar phenomenon has been reported for CTGS[29] under vacuum ultraviolet and UV excitations. Irradiation of high-energy photons may generate the formation of different types of F-center or change the environment of F-centers.

Figure 4 shows the scintillation decay curves under X-ray irradiation. They were approximated by a sum of three exponential functions. The fastest component corresponded to the Instrument Response Function. The two slow components had decay time constants of 0.73 and 7.6 μs for CTGS and 1.2 and 4.1 μs for CTAS. The values were similar to those previously

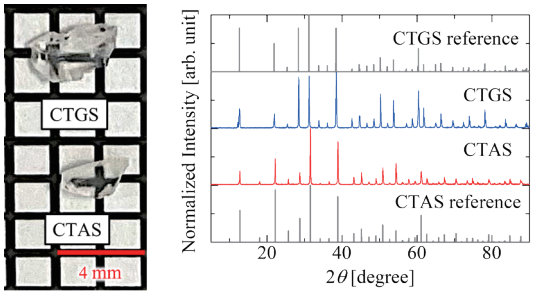

Fig. 1. (Color online) Photograph (left) and XRD patterns (right) of CTGS and CTAS with reference patterns.

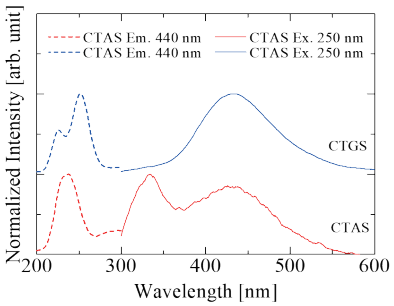

Fig. 2. (Color online) PL excitation (dashed) and emission (solid) spectra of CTGS and CTAS.

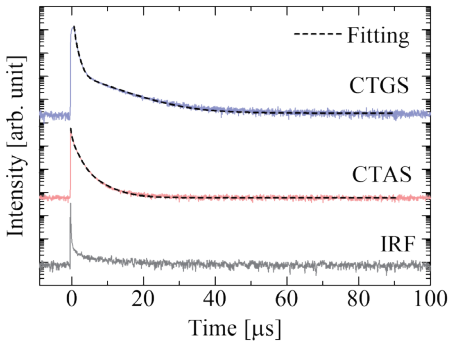

Fig. 3. (Color online) Scintillation spectra of CTGS and CTAS under X-ray irradiation.

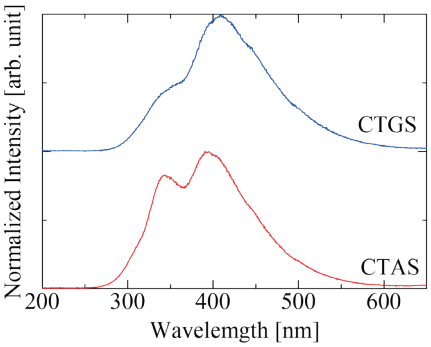

Fig. 4. (Color online) Scintillation decay curves of CTGS and CTAS under X-ray irradiation.

reported for CTGS and another Ta-containing oxide.[19,20,30] The percentages of fast and slow decay components were ~80% and ~20%, respectively. Judging from the intensity ratio presented in Fig. 3, fast and slow components correspond to 400 and 330 nm, respectively.

The afterglow curves of CTGS and CTAS after X-ray irradiation for 2 ms are shown in Fig. 5. The calculation method followed that of our previous study.[31] The calculated *AL*s of CTGS and CTAS were 40 and 30 ppm, respectively, which are significantly better than that of Tl:CsI (268 ppm[21]) calculated by the same method.

Figure 6 shows the PHS of ^{137}Cs γ-rays (662 keV) measured using the prepared CTGS and CTAS, and a reference BGO commercial scintillator. Photoabsorption peaks were observed at 190, 390, and 1550 channels for CTGS, CTAS, and BGO, respectively. The *LY*s of CTGS and CTAS were calculated from the peak channels derived from a single Gaussian approximation and the average quantum efficiencies of the PMT of 34% for CTGS, 35% for CTAS, and 21% for BGO. Consequently, the *LY*s of CTGS and CTAS were 600 and 1200 photons/MeV, respectively. The observed difference can be interpreted using Robbins' model:[32] $LY = S \cdot QY/\beta E_g$, where S, QY, β, and E_g denote the energy transport efficiency, quantum yield at emission centers, eigenvalue of materials, and band gap energies, respectively. β was typically 2.5, and the E_g values of CTGS and CTAS were regarded as nearly identical because their absorption bands appeared at similar wavelengths in transmission spectra in previous studies.[27,28] The obtained *QY*s of CTGS and CTAS were also similar. Therefore, the difference between CTGS and CTAS can be due to *S*, leading to the obtained *LY*s. One hypothesis for the difference in *S* between CTGS and CTAS is follows. The volatilization of a small amount of Ga can occur and generate cation defects during crystal growth, and energy loss due to defects will occur during the energy transport process, which leads to the decrease in *LY*. Compared with other Ta-based compounds such as $YTaO_4$ and $Mg_4Ta_2O_9$,[33,34] the relatively high intensity of the F center emission at 440 nm suggests the presence of more defects, which will lead to a lower *LY* than those of $YTaO_4$ and $Mg_4Ta_2O_9$.

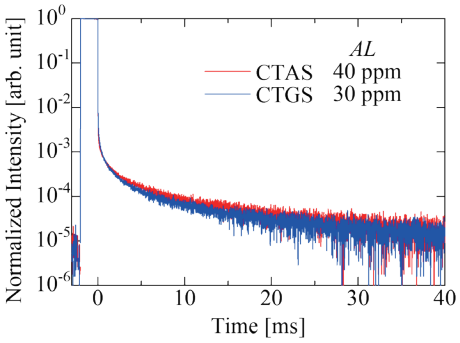

Fig. 5. (Color online) Afterglow curves of CTGS and CTAS samples after X-ray irradiation of 2 ms.

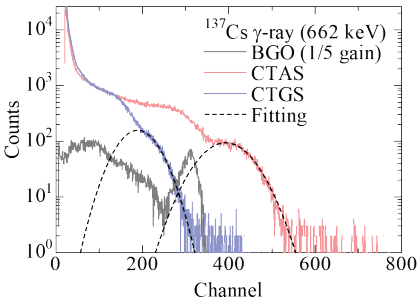

Fig. 6. (Color online) PHS of ^{137}Cs γ-rays measured using CTGS and CTAS samples and reference BGO.

4. Conclusions

In this study, CTGS and CTAS single crystals were synthesized by the FZ method, and their scintillation performances were evaluated and compared. The prepared samples showed emission peaks at 300–600 nm in scintillation spectra under X-ray irradiation, and the scintillation decay time constants were of few ms order. For afterglow properties, the CTGS and CTAS samples showed good *AL*s of 30 and 40 ppm, respectively. However, the *LY*s (CTGS: 600 photons/MeV, CTAS: 1200 photons/MeV) were worse than those of conventional scintillators for integral-type radiation detectors. Comparison of CTGS and CTAS samples showed that their *ALs* were similar, but the *LY* of CTAS was twice that of CTGS. Hence, CTAS is superior as a scintillator. However, since it was not suitable for replacing commercial scintillators, the improvement of its *LY* through mixed crystal formation or dopant introduction will be important.

Acknowledgments

This work was supported by JSPS KAKENHI (Grant nos. 22H00309, 23K25126, 24K03197, and 25K08266), the Cooperative Research Project of the Research Center for Biomedical Engineering, Research Foundation for the Electrotechnology of Chubu, and Shimadzu Science Foundation.

References

1 C. Ronda, H. Wieczorek, V. Khanin, and P. Rodnyi: ECS J. Solid State Sci. Technol. **5** (2016) R3121.
2 S. J. Duclos, C. D. Greskovich, R. J. Lyons, J. S. Vartuli, D. M. Hoffman, R. J. Riedner, and M. J. Lynch: Nucl. Instrum. Methods Phys. Res., Sect. A **505** (2003) 68.
3 L. E. Sinclair, D. S. Hanna, A. M. L. MacLeod, and P. R. B. Saull: IEEE Trans. Nucl. Sci. **56** (2009) 1262.
4 J. Glodo, Y. Wang, R. Shawgo, C. Brecher, R. H. Hawrami, J. Tower, and K. S. Shah: Phys. Procedia **90** (2017) 285.
5 C. L. Melcher, J. S. Schweitzer, R. S. Manente, and C. A. Peterson: IEEE Trans. Nucl. Sci. **38** (1991) 506.
6 C. L. Melcher, J. S. Schweitzer, R. A. Manente, and C. A. Peterson: J. Cryst. Growth **109** (1991) 37.
7 K. Ichiba, T. Kato, D. Nakauchi, N. Kawaguchi, and T. Yanagida: Sens. Mater. **36** (2024) 451.
8 K. Miyazaki, D. Nakauchi, T. Kato, N. Kawaguchi, and T. Yanagida: Sens. Mater. **36** (2024) 515.

9 R. Takahashi, K. Okazaki, D. Nakauchi, T. Kato, N. Kawaguchi, and T. Yanagida: Sens. Mater. **37** (2025) 593.
10 A. Nishikawa, K. Ichiba, T. Kato, D. Nakauchi, N. Kawaguchi, and T. Yanagida: Sens. Mater. **37** (2025) 569.
11 S. Otake, H. Sakaguchi, Y. Yoshikawa, T. Kato, D. Nakauchi, N. Kawaguchi, and T. Yanagida: Sens. Mater. **36** (2024) 539.
12 T. Kato, D. Nakauchi, N. Kawaguchi, and T. Yanagida: Sens. Mater. **36** (2024) 531.
13 S. Otake, S. Takase, T. Kato, D. Nakauchi, N. Kawaguchi, and T. Yanagida: Sens. Mater. **37** (2025) 519.
14 K. Miyajima, A. Nishikawa, T. Kato, D. Nakauchi, N. Kawaguchi, and T. Yanagida: Sens. Mater. **37** (2025) 481.
15 D. Nakauchi, H. Kimura, D. Shiratori, T. Kato, N. Kawaguchi, and T. Yanagida: Sens. Mater. **36** (2024) 573.
16 Y. Takebuchi, A. Masuno, D. Shiratori, K. Ichiba, A. Nishikawa, T. Kato, D. Nakauchi, N. Kawaguchi, and T. Yanagida: Sens. Mater. **36** (2024) 579.
17 K. Okazaki, D. Nakauchi, A. Nishikawa, T. Kato, N. Kawaguchi, and T. Yanagida: Sens. Mater. **36** (2024) 587.
18 E. D. Bourret, D. M. Smiadak, R. B. Borade, Y. Ma, G. Bizarri, M. J. Weber, and S. E. Derenzo: J. Lumin. **202** (2018) 332.
19 R. Takahashi, K. Okazaki, D. Nakauchi, T. Kato, N. Kawaguchi, and T. Yanagida: J. Mater. Sci.: Mater. Electron. **35** (2024) 2139.
20 K. Okazaki, M. Koshimizu, D. Nakauchi, T. Kunikata, T. Kato, N. Kawaguchi, and T. Yanagida: J. Alloys. Compd. **1008** (2024) 176788.
21 D. Nakauchi, T. Kato, N. Kawaguchi, and T. Yanagida: Appl. Phys. Express **13** (2020) 122001.
22 M. J. Weber: J. Lumin. **100** (2002) 35.
23 F. Xue, Y. Hu, L. Chen, T. Wang, and G. Ju: J. Mater. Sci. Mater. Electron. **27** (2016) 8486.
24 D. Nakauchi, G. Okada, N. Kawaguchi, and T. Yanagida: Jpn. J. Appl. Phys. **57** (2018) 100307.
25 T. Yanagida, K. Kamada, Y. Fujimoto, H. Yagi, and T. Yanagitani: Opt. Mater. **35** (2013) 2480.
26 T. Yanagida, Y. Fujimoto, T. Ito, K. Uchiyama, and K. Mori: Appl. Phys. Express **7** (2014) 062401.
27 J. Xin, Y. Zheng, H. Kong, H. Chen, X. Tu, and E. Shi: Cryst. Growth Des. **8** (2008) 2617.
28 X. Fu, E. G. Víllora, Y. Matsushita, Y. Kitanaka, Y. Noguchi, M. Miyayama, K. Shimamura, and N. Ohashi: J. Ceram. Soc. Jpn. **124** (2016) 523.
29 A. P. Kozlova, O. A. Buzanov, V. Pankratova, and V. Pankratov: Low Temp. Phys. **46** (2020) 1178.
30 M. Serhan, M. Sprowls, D. Jackemeyer, M. Long, I. D. Perez, W. Maret, N. Tao, and E. Forzani: CrystEngComm **22** (2020) 3497.
31 R. Takahashi, K. Okazaki, D. Nakauchi, T. Kato, N. Kawaguchi, and T. Yanagida: Opt. Mat. **164** (2025) 117064.
32 D. J. Robbins: J. Electrochem. Soc. **127** (1980) 2694.
33 O. Voloshyna, S. V. Neicheva, N. G. Starzhinskiy, I. M. Zenya, S. S. Gridin, V. N. Baumer, and O. Ts. Sidletskiy: Mater. Sci. Eng., B **178** (2013) 1491.
34 T. Hayashi, K. Ichiba, D. Nakauchi, K. Watanabe, T. Kato, N. Kawaguchi, and T. Yanagida: J. Lumin. **255** (2023) 119614.